MICROCOPY   CHART

The Orientation Distribution of Nonspherical

Aerosol Particles within a Cloud

Final Technical Report

by

Isaiah Gallily
Chief Investigator

Department of Atmospheric Sciences
The Hebrew University of Jerusalem

Jerusalem, Israel

December,1985

86 5 8 017

The Orientation Distribution of Nonspherical

Aerosol Particles within a Cloud

Final Technical Report

by

Isaiah Gallily
Chief Investigator

Department of Atmospheric Sciences
The Hebrew University of Jerusalem

Jerusalem, Israel

December,1985

SECURITY CLASSIFICATION OF THIS PAGE (When Data Entered)

REPORT DOCUMENTATION PAGE	READ INSTRUCTIONS BEFORE COMPLETING FORM

1. REPORT NUMBER	2. GOVT ACCESSION NO.	3. RECIPIENT'S CATALOG NUMBER
	AD-A167 326	

4. TITLE (and Subtitle)	5. TYPE OF REPORT & PERIOD COVERED
The Orientation Distribution of Non-spherical Aerosol Particles within a Cloud	Final Technical Report
	6. PERFORMING ORG. REPORT NUMBER

7. AUTHOR(s)	8. CONTRACT OR GRANT NUMBER(s)
Dr. Isaiah Gallily	DAJA45-83-C-0004

9. PERFORMING ORGANIZATION NAME AND ADDRESS	10. PROGRAM ELEMENT, PROJECT, TASK AREA & WORK UNIT NUMBERS
Department of Atmospheric Sciences The Hebrew University of Jerusalem	61102A 1T161102BH57-01

11. CONTROLLING OFFICE NAME AND ADDRESS	12. REPORT DATE
USARDSG-UK Box 65, FPO NY 09510	December 1985
	13. NUMBER OF PAGES
	32

14. MONITORING AGENCY NAME & ADDRESS(If different from Controlling Office)	15. SECURITY CLASS. (of this report)
	Unclassified
	15a. DECLASSIFICATION DOWNGRADING SCHEDULE

16. DISTRIBUTION STATEMENT (of this Report)

Approved for public release; distribution unlimited.

17. DISTRIBUTION STATEMENT (of the abstract entered in Block 20, if different from Report)

18. SUPPLEMENTARY NOTES

19. KEY WORDS (Continue on reverse side if necessary and identify by block number)

Orientation of Nonspherical Aerosol Particles

20. ABSTRACT (Continue on reverse side if necessary and identify by block number)

The orientation distribution of non-spherical particles within a cloud was studied. Theoretically, the subject was treated for a general laminar flow of intermediate as well as weak and strong character, and for a turbulent flow whose Kolmogoroff scale was much larger than the particles themselves. The laminar flow served as one realization for the turbulent field within

DD FORM 1473 EDITION OF 1 NOV 65 IS OBSOLETE

the cloud.

It is found that the orientation distribution function in a laminar medium is generally structured with a preferred orientation while that of the turbulent medium is random on the average but with a significant dispersion.

Experimentally, a horizontal wind tunnel was erected for orientation measurements; it was equipped with a dedicated hot-wire computerized system for turbulence characterization, which was shown to conform to the determinations of Laufer. Light scattering signals were used as the orientation-gauge.

I. INTRODUCTION

The orientation distribution function F of nonspherical particles is of great importance for the evaluation of system properties with a directional dependence. In the transport mechanics field of interest, the mean settling velocity of a cloud of orientable particles (1), and the particle-ensemble orientationally averaged diffusion tensor (2-[?]) serve as examples of a property determined by F. Also, the optical-orientation interaction in a system of morphologically unisotropic particles (5-7) constitutes another case of this behavior. The orientation distribution of nonspherical particles or molecules in solution, which is essentially the same phenomenon, has been a major subject of interest in rheology for a long time.

In essence, the orientation of particles in space depends on the interplay between a randomizing action such as that of rotational Brownian motion and microturbulence, and an orienting action arising from fluid dynamic field gradients and external torques; likewise, the orientation can be affected by a (physical) concentration source due to translational diffusion of the particles (8).

In the frequently encountered cases characterized by the absence of external orienting forces and by a (concentration) source whose contribution can be ignored due to the small value of the ratio between a typical particle size and system's dimension (9), and for laminar flows, the orientation distribution function F will be determined only by the flow gradient and particles' rotational Brownian motion. The relative weight of these factors is expressed in the rotational Peclet number α defined by $\alpha = W_0/D_0$ where W_0 is a typical gradient and D_0 is a typical rotational diffusion coefficient. Essentially, the function F is a flow property.

Studies on the nature of the distribution function have been carried out for cases of spheroidal particles immersed in a special though representative in certain situations flow like that of a simple shear (10,11) and an irrotational extensional one (12). Also, investigations have been performed for the asymptotic situations of a very strong field, $\alpha \gg 1$, and a very weak field $\alpha \ll 1$, and nearly spherical particles (8,13).

The interest in rheology was mostly in the second moment of the particle orientation vector $\mathbf{p}$; so, for the intermediate cases of α, it was sufficient (14) to use a closure interpolation technique based on the solution for the asymptotic situations, and construct approximate constitutive equations for $\langle \mathbf{pp} \rangle$ rather than find the function F itself. The derivation of the latter function, from which the moments f any orientation-dependent quantity can be deduced, is very desriable but extremely complex for intermediate values of a (14); it has not been achieved up to now for these α-cases and for a general shear flow.

AIM OF STUDY

Since many aerosol systems in closed regions involve intermediate Peclet numbers and multidimensional flows where all nine components of the gradient tensor W may be present, and as many of the systems contain particles varying in their typical aspect ratio over a wide range, it was worthwhile to undertake a study aimed to obtain the orientation distribution function F for such situations. In general, we planned to conduct the research according to the accepted picture of a turbulent uni (or multi)-phase medium. In this picture, the turbulent field average properties are assumed to be created by the contribution of (theoretically) an infinite number of the so-called "realizations" in each of which the motion of a fluid element or a particle at every space-time point is uniquely defined.

Thus, it was natural to divide our study into the following three parts:

1. A (theoretical) analysis of the orientation behavior of model
           nonspherical aerosol particles within one "realization"
        which is characterized by a laminar medium, in essence,

2. A (theoretical) analysis of the orientation behavior of the
        above particles within a turbulent field, with a special emphasis
        on the lower atmospheric boundary layer and a turbulent jet,

3. An experimental test of the theoretical conclusions by some effect
        such as light-scattering .

In this stage of the study, it was reasonable to concentrate on the case of axisymmetric particles such as spheroids with an aspect ratio $R(=a_1/a_2)$ of $0 < R < \infty$.

Needle-like prolate particles may simulate asbestos fibers and straight-chain aggregates while disk-like oblate particles may represent mineral platelets, thus, though the problem of modelling of real (geometrically impure) shapes of nonspherical aerosol particles by regular forms is still unsolved in general, the above axisymmetric shapes can serve as useful approximations.

In passing, it should be stressed that the herewith reported research was devoted to such a case in which the particles could be considered as moving in a continuous fluid. The other cases such as that of particles comparable in (typical) size to the mean free-path of the (gaseous) medium is not amneable as yet to a (sufficiently) exact analysis.

II . THE LAMINAR, ONE "REALIZATION" CASE

1. Mathematical Formulation of the Problem

Consider a system of small spheroidal particles embedded in a general shear laminar flow $\mathbf{u}$ which can be given in their vicinity by [1]

$$\mathbf{u}(x,t) = \mathbf{W}(t) \cdot \mathbf{x}. \tag{2.1}$$

The distribution function F is described, in orientation space and with the justifiable neglect of a concentration source (see above), by the known Fokker-Planck equation

$$\frac{\partial F}{\partial t} + \nabla \cdot (F\omega - \mathbf{D} \cdot \nabla F) = 0 \tag{2.2}$$

where ω is particle's rotational velocity.

In the following text the components of ω for rotational ellipsoids in the general laminar flow of (2.1) are given in part **2** , which can be viewed as a preliminary treatment; then, the solution of Eq. (2.2) for such a flow is presented in part **3** , and numerical experiments for interesting cases are brought out in part **4** .

----

[1]For nomenclature see APPENDIX A .

2. The Rotational Velocity Components in A general Shear Flow

In order to solve the Fokker-Planck equation for F in a general flow field, one has to know the dependence of the rotational velocity ω on $\mathbf{W}$.

The components ω for ellipsoidal particles in a creeping flow were calculated by Jeffery (15) in general but were specifically given by him only for the rotational bodies in a simple shear flow. These components were later obtained by Hinch and Leal (16) for any ellipsoid though also only for the above kind of flow. On the other hand, Takserman-Krozer and Ziabicki (12) presented expressions for irrotational flows which hold however solely for the axisymmetric case. Thus to find the components of ω in the general shear flow we had to proceed in the following way:

Let us take a rectangular coordinate system x_k fixed in space and a (rectangular) one x'_k locked in the particle with Euler angles θ, φ, ψ, such that θ is the angle between x'_1 and x_1, φ is the angle between the planes $x_1 x_2$ and $x_1 x'_1$ and ψ is the angle between the planes $x_1 x'_1$ and $x'_1 x'_2$ (Fig.1). Then the transformation matrix between the two systems x_k and x'_k will be given by

$$B = \begin{vmatrix} c\theta & s\theta c\varphi & s\theta s\varphi \\ -s\theta c\psi & \begin{matrix} -s\varphi s\psi \\ +c\theta c\varphi c\psi \end{matrix} & \begin{matrix} c\varphi s\psi \\ +c\theta s\varphi c\psi \end{matrix} \\ s\theta s\psi & \begin{matrix} -s\varphi c\psi \\ -c\theta c\varphi s\psi \end{matrix} & \begin{matrix} c\varphi c\psi \\ -c\theta s\varphi s\psi \end{matrix} \end{vmatrix} \qquad (2.3)$$

Kinematically the components of ω in the x'_k system are related to the Euler angles and their temporal change by

$$\omega_1 = \dot{\varphi}c\theta + \dot{\psi} ,$$
$$\omega_2 = \dot{\theta}s\psi - \dot{\varphi}s\theta c\psi ,$$
$$\omega_3 = \dot{\theta}c\psi + \dot{\varphi}s\theta s\psi$$

$$(2.4)$$

where $c\theta$ is $\cos\theta$, $s\theta$ is $\sin\theta$ and similarly for φ and ψ; likewise, the components for sufficiently small ellipsoids and with the neglect of torques are expressed by Jeffery's general relationship (15)

$$\omega_i = \frac{1}{2}[V'_{kj} + S'_{kj}(a_j^2 - a_k^2)/(a_j^2 + a_k^2)] \tag{2.5}$$

where $i, j, \kappa \rightarrow 1, 2, 3$ are cyclic permutation indices, a_i, a_j, a_κ are the semi-axes of the ellipsoids and the vorticities V'_{ij} and the strain coefficients S'_{ij} are defined by

$$V'_{ij} = W'_{ij} - W'_{ji} \quad , \quad S'_{ij} = W'_{ij} + W'_{ji} \tag{2.6}$$

for the assumed gradient field in which

$$W'_{ij} = \frac{\partial u'_i}{\partial x'_j} \tag{2.7}$$

In this case of small ellipsoids, Eq. (2.5) should hold even for non-uniform slow motions of the particles if the typical time of change of $W(t)$ of (2.1) is large enough in comparison with the relaxation time of the latter.

By the similarity transformation from x_κ to x'_κ we have

$$W'_{ij} = B_{ik} W_{kl} B^{-1}_{lj} \tag{2.8}$$
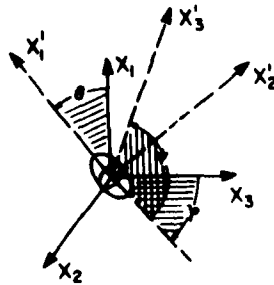
where the repeated index implies summation.

Fig.1. The Euler angles and two systems of coordinates.

So Eqs. (2.4), (2.5) and (2.8) for rotational ellipsoids with $a_2 = a_3$ lead to the final expressions.

$$\dot\varphi = V_{32}/2 + ctg\Theta(E_{31}c\varphi - E_{21}s\varphi) + \lambda\left(\frac{1}{2}S_{32}c_2\varphi - Q_1 s_2\varphi\right),$$

and

$$\dot{\theta} = G_{2131} c^2\theta - G_{1213} s^2\theta + \frac{\lambda}{2} s_2\theta \left(Q_2 + Q_1 c_2\varphi + \frac{1}{2} S_{32} s_2\varphi\right). \tag{2.9}$$

Here, for brevity sake, we denote

$$E_{ik} = \frac{1}{2}\left(V_{ik} + \lambda S_{ik}\right),$$

$$G_{ijkl} = E_{ij} c\varphi + E_{kl} s\varphi.$$

$$Q_1 = \frac{1}{2}\left(W_{22} - W_{33}\right), \qquad Q_2 = \frac{1}{2}\left(W_{22} + W_{33} - 2W_{11}\right),$$

$$V_{ik} = W_{ik} - W_{ki} \quad , \qquad S_{ik} = W_{ik} + W_{ki} \; , \tag{2.10}$$

$$W_{ik} = \frac{\partial u_i}{\partial x_k} \quad ,$$

$$c_m\theta = \cos m\theta, \quad c^m\theta = \cos^m\theta, \quad s_m\theta = \sin m\theta, \quad s^m\theta = \sin^m\theta.$$

and similarly for φ ; λ is defined by $\lambda = (R^2-1)/(R^2+1)$.

The special cases of the previously studied flows and axisymmetric particles are readily deduced from the above equations. Thus, Jefferey's frequently used solution (15) for a Couette flow $(0,0,q x_2)$ follows from (2.7)-(2.8) as

$$\dot{\varphi} = \frac{1}{2}\left(V_{32} + \lambda S_{32} c_2\varphi\right) = \frac{1}{2} q(1 + \lambda c_2\varphi)$$

and

$$\dot{\theta} = \frac{\lambda}{4} S_{32} s_2\theta s_2\varphi = \frac{\lambda}{4} q s_2\theta s_2\varphi. \tag{2.11}$$

Likewise, for the irrotational flow characterized by

$$W_{22} = W_{33} = -W_{11}/2 = -q/2 \tag{2.12}$$

and all other W_{ik} equal to zero, we get

$$\dot{\varphi} = 0, \quad \dot{\theta} = \frac{\lambda}{2} Q_2 s_2 \theta = -\frac{3}{4} \lambda q s_2 \theta, \tag{2.13}$$

which are in agreement with Takserman-Krozer and Zibabicki (12).

3. The Solution for the Orientational Distribution Function

Let us designate by W_o a velocity gradient typical of the considered problem, and introduce the dimensionless parameters

$$\tilde{W}_{ik} = W_{ik}/W_o, \quad \tilde{t} = W_o t. \tag{2.14}$$

then, the diffusion equation (2.2) together with (2.4),(2.9)and (2.14) can be written as

$$\frac{\partial F}{\partial t} + \frac{1}{\sin\theta} \frac{\partial}{\partial\theta} (F\dot{\theta}\sin\theta) + \frac{\partial}{\partial\varphi} (F\dot{\varphi}) = \Delta F/\alpha \tag{2.15}$$

where the rotational Peclet number α is defined as before by $\alpha = W_o/D$, and D now is the mid-diameter rotational diffusion coefficient; the sign $\sim$ is henceforth dropped out for simplicity.

The normalization condition is taken as usual to be

$$\int_0^{2\pi} \int_0^{\pi} F\sin\theta d\theta d\varphi = 1. \tag{2.16}$$

According to the theory of Fourier series, one can obtain the solution of (2.15) in the form

$$F = \sum_{n=0}^{\infty} \sum_{m=0}^{\infty} \left(1 - \frac{1}{2}\delta_{mo}\right)\left[A_{on}^m(t)c_m\varphi + A_{1n}^m(t)s_m\varphi\right] P_n^m(c\theta) \tag{2.17}$$

as long as the equation for F has a Laplacian in θ and φ. Such a function, which is twice differentiable with regard to these variables, can be uniformly approximated at every moment t by a finite series of the orthogonal spherical harmonics.

Inserting (2.1.7) in (2.15) and taking into account the symmetry properties of F based on physical reasoning, one gets for $A_{kn}^{m}(t)$

$$\frac{dA_{kn}^{m}(t)}{dt} = -\frac{n(n+1)}{\alpha} A_{kn}^{m} - \sum_{j=n-2}^{n+2} \sum_{p=m-2}^{m+2} \sum_{l=1}^{2} (1+\delta_{mo})$$

$$\times \left[D_{l,jn}^{pm} A_{kj}^{p} + (-1)^{k} C_{l,jn}^{pm} A_{1-k,j}^{p} \right] \qquad (2.18)$$

where $k = 0.1$, $n = 2,4 \cdots$, and $m = 0,1,2, \cdots n$.

The expressions for the coefficients $D_{l,jn}^{pm}$ and $C_{l,jn}^{pm}$ appearing in (2.18) are given in Table 1. The vorticities V_{ik}, the strains S_{ik}, and Q_1, Q_2 are defined by (2.10); the indices j and n are even. The numerical coefficients d_{jn}^{pm} can be calculated from Table II according to the position indicated in the last column of Table I. In Table II $e_1 = 1/[2(2n-1)(2n+1)]$,

$e_2 = 1/[2(2n-1)(2n+3)]$, and $e_3 = 1/[2(2n+1)(2n+3)]$;

all other $d_{nn'}^{mm'}$ coefficients including those of negative indices and those related to index combinations not appearing in the table, are zero. The corresponding $D_{l,jn}^{pm}$ and $C_{l,jn}^{pm}$ coefficients fall out too. The value of $A_{oo}^{o} = 1/2\pi$ can be obtained from the normalization condition (2.16) and $A_{1n}^{o} = 0$ since sin $m\varphi = 0$ for $m = 0$. Here it should be noted that for the steady-state situation, when $\partial F/\partial t = 0$, the r.h.s. of the general equations (2.18) provides recurrence relations for A_{on}^{m} and A_{1n}^{m} which include those of the previously studied special cases.

TABLE I
The Coefficients $D_{l,jn}^{pm}$ and $C_{l,jn}^{pm}$

l	p	m	$D_{l,jn}^{pm}$	$C_{l,jn}^{pm}$	Location of d_{jn}^{pm} in Table II
1	$m \pm 1$	1, 2, 3 $\cdots$	$\delta_m(p-m)V_{12}/4 + \lambda d_m^{pm}S_{12}$	$\delta_m V_1\sqrt{}/4 + (p-m)\lambda d_m^{pm}S_{11}$	I
2	$m \pm 2$	0, 2, 4 $\cdots$	$\lambda d_m^{pm}[2Q_1(1-\delta_{mo}) + Q_2\delta_{mo}\delta_{po}]$	$m\delta_{po}\delta_{pm}V_{32}/2 + (p-m)\lambda d_m^{pm}S_{32}/2$	If $p = m = 0$ III Else II

Now, just to compare our solution with some of the former studies, let us take the stationary gradient field with perpendicular and parallel components

$$\mathbf{W} = \begin{vmatrix} W_{11} & 0 & 0 \\ 0 & W_{22} & W_{23} \\ 0 & W_{32} & W_{33} \end{vmatrix} \tag{2.19}$$

which includes as special cases simple shear and extensional flows. Considering the field of (2.19), small enough λ values, and truncating (2.17) and (2.18) at $n \leqslant N = 2$, one obtains for the first terms of the steady-state solution as expanded in λ

$$F = \frac{1}{4\pi} \left\{ 1 - \frac{\lambda Q_2 (3c^2\theta - 1)}{2(3/\alpha + \lambda Q_2)} + \frac{3\lambda s^2\theta}{2(36/\alpha^2 + V_{32}^2)} \right.$$
$$\left. \times \left[\left(\frac{12}{\alpha} Q_1 - S_{32} V_{32}\right) c_2\varphi + 2\left(\frac{3}{\alpha} S_{32} + Q_1 V_{32}\right) s_2\varphi \right] + \cdots \right\}. \tag{2.20}$$

Thus, for the Couette flow $(0,0,qx_2)$, when only W_{32} is not equal to zero, the solution described by (2.20) coincides with that of Peterlin (10) in the first order of λ if one takes into account the convention difference of signs and puts in (2.14) $W_o = q$. Also in the case of the irrotational flow of (2.12), we get by an expansion in $\lambda\alpha$ an accord with Takserman Krozer and Ziabicki (12).

These agreements could be anticipated on the grounds that the corresponding coefficients

TABLE II

The Numerical Coefficients $d_{nn'}^{mm'}$

n'	m'	I	m'	II	m'	III
$n-2$	$m-1$	$-e_1(n-2)\prod_{i=0}^{2}(n+m-i)$	$m-2$	$\frac{e_1}{2}(n-2)\prod_{i=0}^{3}(n+m-i)$	0	$-e_1\prod_{i=0}^{2}(n-i)$
n	$m-1$	$3e_2(2m-1)/2$	$m-2$	$\frac{3e_2}{2}\prod_{i=1}^{2}(n-m+i) \times (n+m-i+1)$	0	$e_2 n(n+1)$
$n+2$	$m-1$	$-e_3(n+3)\prod_{i=1}^{3}(n-m+i)$	$m-2$	$-\frac{e_3}{2}(n+3)\prod_{i=1}^{4}(n-m+i)$	0	$e_3\prod_{i=1}^{3}(n+i)$
$n-2$	$m+1$	$e_1(n-2)(n+m)$	$m+2$	$e_1(n-2)/2$		
n	$m+1$	$3e_2(2m+1)/2$	$m+2$	$3e_2/2$		
$n+2$	$m+1$	$e_3(n+3)(n-m+1)$	$m+2$	$-e_3(n+3)/2$		

$D_{L,jn}^{pm}$, $C_{L,jn}^{pm}$ in Tables I and II are in harmony with those of the recurrence relations of both the latter studies. Obviously, for arbitrary prameters λ, α, and W_{ik} one has to take a sufficiently large N which requires the use of the computer.

4. Numerical Results

The investigated particles were long prolate ellipsoids of aspect ratio $5 \leqslant R \leqslant 10^3$ and thin oblate spheroids of aspect ratio $0.01 \leqslant R \leqslant 0.1$ which can, respectively, simulate long cylinders and thin platelets. The average characteristic dimension of these particles was taken to be $r \sim 10^{-5} - 10^{-3}$ cm; so their rotational mid-diameter diffusion coefficient, as calculted from the classical expressions(see Gans (17), was $D \sim 1 \sec^{-1}$. The typical flow velocities of interest were assumed to be 1-10 m $\sec^{-1}$ and the typical velocity gradients 1-10 $\sec^{-1}$, all of which correspond to Peclet numbers of $\alpha \sim 1$-10.

We considered various models of flow which enabled us to study possible effects on the orientation of the aerosol particles in closed environment and atmospheric conditions. The initial orientation of the particles was taken as random; the field W_{ik} could be either stationary or nonstationary. In the last case, the components W_{ik} were supposed with no loss of generality to vary with time, with a frequency Ω and initial phase β as $\cos(\Omega t + \beta)$.

The system (2.18) for $A_{kn}^{m}(t)$ was treated by a high-accuracy differential equations-solver based on the extrapolation method of Burlish and Stoer (18). All the summation operations in the r.h.s. of (2.18) as well as in (2.17) were carried out with double precision. The program was checked against the solution for F obtained by Peterlin (10) and Takserman-Krozer and Ziabicki (12) for the above cited special cases. For stationary flows and sufficiently large t when a steady state is being reached, our solution coincided with that achieved by us also through the Gauss elimination method applied with double precision. This has been carried out to test the computational compatibility of different methods in treating the system of (2.18).

A fast enough convergence of the solution for F with a reasonable accuracy has been achieved as a rule. The calculations were carried out for $\alpha = 1$ with $n \leqslant N = 4,6$ (n,N-even) which coincided to up to four decimals and better with solutions where a higher value of N was adopted; for $\alpha = 10$, we used N = 10-14 and got an accuracy for maximum and mean values of better than 1% which was considered quite satisfactory for our purposes. In the case of $|\lambda| \leqslant 0.923$ $(0.2 \leqslant R \leqslant 5)$ or some fields of W_{ik} smaller values of N could be taken.

Of the (physical) situations which were considered, we bring here these of:

> a. A point source

and

> b. A circular laminar jet

A point source flow

We consider here a flow created by a point source, where the velocity is given by $u = q_0 r / 4\pi r^3$ and its gradients are

$$W_{ik}^{(3)} = \frac{\delta_{ik}}{r^3} - \frac{3 x_i x_k}{r^5} \tag{2.21}$$

with $W_0 = q_0 / 4\pi r_0^3$. In Eq. (2.21) x_i is nondimensionalized by a typical length r_0, $r(x_i)$ is the radius vector and q_0 a constant. $W_{ik}^{(3)}$ is considered to be constant in the immediate neightborhood of the (small) particles.

The orientation distribution function F for such a flow is presented in Fig. 2 as $F(\theta, \varphi)$ vs θ for $\varphi = 0, \pi/4$; $\alpha = 1$; $R = 50 (\lambda \approx 1)$; and $R = 0.02 (\lambda \approx -1)$, a platelet), and for the (arbitrary) space point $x_1 = 1$, $x_2 = x_3 = 0.4$. At this point we have

$$W^{(3)} = \begin{pmatrix} -.840 & -.599 & -.599 \\ -.599 & .420 & -.240 \\ -.599 & -.240 & .420 \end{pmatrix}. \tag{2.22}$$

From Fig. 2 it can be seen that, as soon as the components of $W^{(3)}$ decrease with distance and become mostly negative, the location of the maxima of F for cylindrical and plateletlike particles change to values of θ and φ opposite to those of the former cases of fields $W^{(1)}$ and $W^{(2)}$. In Fig. 3 are brought out curves of the maximal values of F, F_m, as a function of time t for various particle aspect ratios $0.02 \leqslant R \leqslant 50$, $1 \leqslant \alpha \leqslant 10$, and for the same space points as of Fig. 2. The positions of the first maxima in F are shown too. An important point to be noted in this flow case is that the orienting action of the velocity gradient (2.22) is noticeably stronger for platelets (curves 1,2) than for cylinders (curves 7,8) at $\alpha = 10$ but that this difference is weakened with the decrease of α.
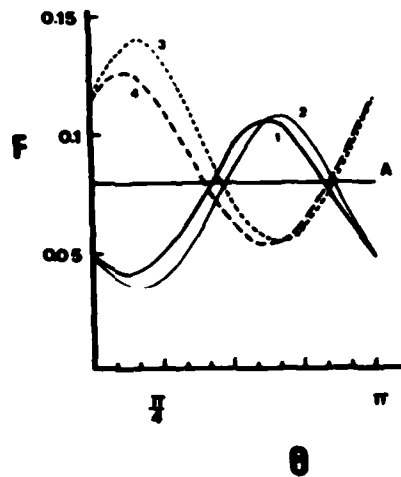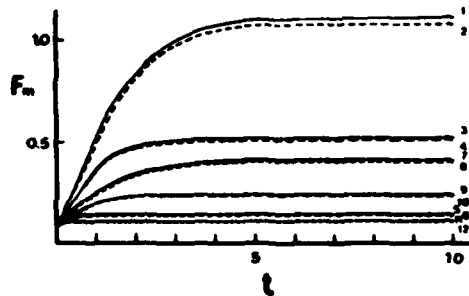
Fig. 2 . The orientation distribution function F vs θ for the
point source gradient $W_{ik}^{(3)}$ of (2.21) , $\alpha =1,R =0.02$
(platelets) and R = 50 (long cylinders) $t \geqslant 2$; $x_1 =1, x_2 = x_3 = 0.4$.
$A - t = 0$; ———, R = 50: 1. $\varphi = 0$, 2. $\varphi = \pi/4$; ---, R = 0.02 : 3. $\varphi = 0$,
4. $\varphi = \pi/4$.

1. $\alpha = 10$, $R = 0.02$
2. $\alpha = 10$, $R = 0.1$
3. $\alpha = 5$, $R = 0.02$
4. $\alpha = 5$, $R = 0.1$
5. $\alpha = 1$, $R = 0.02$
6. $\alpha = 1$, $R = 0.1$

$\theta_m = \pi/6$
$\varphi_m = \pi/4$
$(t \geqslant 1)$

7. $\alpha = 10$, $R = 50$
8. $\alpha = 10$, $R = 10$

$\theta_m = 3\pi/4$
$\varphi_m = \pi/4$
$(t \geqslant 2)$

9. $\alpha = 5$, $R = 50$
10. $\alpha = 5$, $R = 10$
11. $\alpha = 1$, $R = 50$
12. $\alpha = 1$, $R = 10$

$\theta_m = 2\pi/3$
$\varphi_m = \pi/4$
$(t \geqslant 1)$

Fig. 3 F_m vs. t for a point source gradient $W_{ik}^{(3)}$ (2.21)
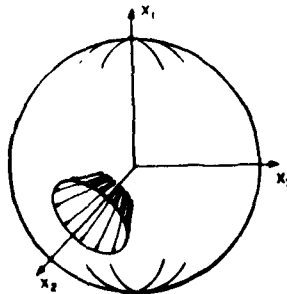with $x_1 = 1$, $x_2 = x_3 = 0.4$.

Fig. 4 A perspective view of particle orientation in a point source field
(schematical) .

A circular laminar jet

The velocities within a circular laminar jet are given by Schlichting (19) as

$$u_1 = \frac{2\delta^2 \nu}{x_1} f(\xi), \qquad u_\tau = \frac{\delta \nu \xi}{x_1}(1 - \xi^2/4) f(\xi) \qquad (2.23)$$

where $\xi = \gamma r/x_1$, $f(\xi) = (1 + \xi^2/4)^{-2}$ .Here ν is the kinematic viscosity,γ is determined by the jet momentum $J = \frac{16}{3}\pi\rho\gamma^2\nu^2$, ρ density, and r is the radial distance; τ and x_1 are nondimensionalized later on by r_o again.

For this flow, the components of $W(x_1, \tau)$ are

$$W_{11} = -\eta(1 - 3\xi^2/4), \quad W_{1r} = -\delta\eta\xi, \quad W_{\tau 1} = W_{11}\xi/\gamma,$$

$$W_{\tau\tau} = \frac{1}{2}\eta\left(1 - \frac{3}{2}\xi^2 + \frac{\xi^4}{16}\right) + \frac{u_\tau}{\tau} \qquad (2.24)$$

with $\eta = 2\gamma^2\nu/[x_1^2(1+\xi^2/4)^3]$; they are taken to be constant in the vicinity of the (small) particles as in the point source case.

The dependence of F on Θ at $\varphi = 0, \pi/4$ is presented in Fig.5 for the indicative case of $\alpha = 1, \gamma = 1$, various particle aspect ratios R, the space point $x_1 = 1$ $\xi = 0.5$, $x_2 = x_3$, and $W_o = \alpha D = 2\gamma^2\nu/r_o^2$. Here the velocity gradients which decrease with the distance too, are (in Cartesian coordinates x_k)

$$W^{(4)} = \begin{pmatrix} -.678 & -.295 & -.295 \\ -.239 & .339 & -.077 \\ -.239 & -.077 & .339 \end{pmatrix}$$

$$(2.25)$$

and thus one can conjecture that the character of the orientation distribution function of platelets and cylinders would be similar to that of the point source case.

A perspective, schematical illustration of the orientation in the jet's field is shown in Fig. 6 which is constructed with the consideration on the jet's axial symmetry.
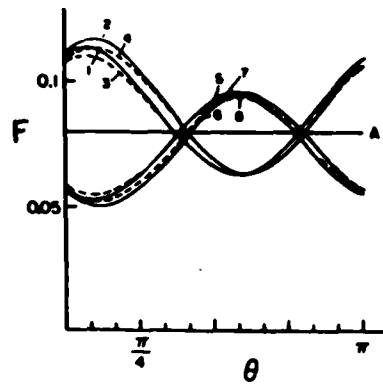
Fig. 5. The orientation distribution function F vs. Θ in a flow of
axisymmetric laminar jet (2.24)-(2.25) at $x_1 = 1$, $x_2 = x_3$, $\xi = 0.5$,
for platelets and cylinders at R = 0.01, 0.2, 5, 100; $\varphi = 0, \pi/4$; $\alpha = 1, \gamma = 1, t \geqslant 2$.
1. $R = 0.01, \varphi = 0$;   3. $R = 0.2, \varphi = 0$;   5. $R = 100, \varphi = 0$;   7. $R = 5, \varphi = 0$;
2. $R = 0.01, \varphi = \pi/4$;   4. $R = 0.2, \varphi = \pi/4$;   6. $R = 100, \varphi = \pi/4$;   8. $R = 5, \varphi = \pi/4$.
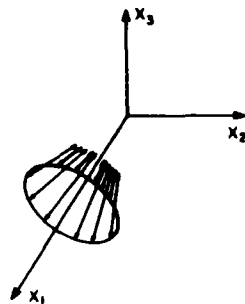

Fig. 6. A perspective view of particle orientation in a laminar jet field
(schematical)

The computer code for the (steady)laminar, one"Realization" case is deposited
with the CDRC, Aberdeen Proving Ground, MD., c/o Dr. J. Buttiger.

5. Interim Conclusions

Obviously, we did not intend in this study to cover every significant case of a particle assembly; however, the type of particles and flow fields covered by us and given here is very conductive to the prediction of the behavior of real and important systems. The following conclusions can be drawn out:

(i) The method put forth in this study provides a useful and convenient tool in the structure analysis of the orientation distribution function F for a wide class of particle parameters and flow configurations. In practical use, the obtained solution converged fast enough.

(ii) The solution for F achieved here includes as special cases those of previous studies.

(iii) The character of F has some regularities distinguished by perceptible maxima whose values and locations can be found in a general shear flow; these maxima will give clear indication of a preferred orientation.

(iv) The time evolution of F, the time relaxation, and, correspondingly, other integral characteristics of it can be determined now with sufficient accuracy.

(v) The positions of the maxima of F are established fairly fast and do not change appreciably with time.

(vi) Significant differences exist in the orientational effect regarding the maximum values of F for platelets and long cylinders in different flow situations; the effect is stronger for platelets than for cylinders in velocity gradient fields which decrease with distance.

- 16 -

APPENDIX A : NOMENCLATURE

a_i semi-axes of ellipsoidal particle (a_1 ,lies along x_1)

A   transformation matrix with component A_{ik}

A^m_{on} , A^m_{1n} coefficients in expansion of F, Eq. (2.17)

B   transformation matrix with components B_{ik} , Eq. (2.3) ; B^{-1}_{ik} components of inverse matrix

$c_m\theta$ $\cos m\theta$,and the same for φ and ψ ; $c^m\theta$ $\cos^m\theta$,and the same for φ and ψ ; $C^{pm}_{l,jn}$, $D^{pm}_{l,jn}$ coefficients in Eqs. (2.18) and Table 1

D   rotational diffusion tensor of the particle; D rotational diffusion coefficient around a mid-diameter

E_{ik} defined in text, Eq. (2.10)

e_1, e_2, e_3 coefficients, Table II

F   orientation distribution function ; F_m , maximal value of F

G_{ijkl} defined in text. Eq. (2.10)

i, j, k, l running indices

m, m'

n, n', p

J   jet's momentum

N   upper limit of n in Eqs. (2.17) and (2.18)

P^m_n associated Legendre polynomial

q   velocity gradient

q_o constant

Q_1, Q_2 functions of fluid flow. Eq. (2.10)

R   particle's aspect ratio $R = a_1/a_2$

r_o typical length

S_{ij} strain coefficients referred to coordinate system x_k ; S'_{ij} coefficients referred to system x'_k

$s_m\theta$ $\sin m\theta$ and   the same for φ and ψ

$s^m\theta$ $\sin^m\theta$ and   the same for φ and ψ

t time

$\mathbf{u}$ fluid velocity; u_i' components in coordinate system locked into the particle x_k'

V_{ij} vorticity coefficients referred to system x_k, V_{ij}' coefficients referred to system x_k'

$\mathbf{W}$ velocity gradient tensor ; W_{ik} components of tensor referred to system x_k ; W_{ik}' components referred to x_k', W_o , typical velocity gradient

x_k (k=1,2,3) Cartesian coordinates fixed in space

x_k' coordinate fixed in the particle

Greek Letters

α rotational Peclet number

β initial phase

γ constant determined by the jet's momentum J

δ Kronecker's delta

θ, φ, ψ Euler's orientational angles ; θ_m , φ_m are positions of F_m

λ dimensionless particle parameter defined by $\lambda = (R^2-1)/(R^2+1)$

ω rotational velocity of the particles with components ω_i

Ω frequency

APPENDIX B : REFERENCES

1. Brenner, H. and Happel J. "Low Reynolds Number Hydrodynamics, "Chaps.5-8 Prentice-Hall, Englewood Cliffs, N.J. 1965.

2. Brenner, H. and Condiff, D.M. J. Colloid Interface Sci. 41, 228 (1972)

3. Eisner, A.D. and Gallily, I. J. Colloid Interface Sci. 81, 214 (1981)

4. Eisner, A.D. and Gallily, I. J. Colloid Interface Sci. 88,185 (1982)

5. Heller, W. Wada, E. and Papazian,L.A. J. Polym. Sci. 47,481 (1961)

6. Okano, K. and Wada E.J. Chem. PHys 34,405 (1961).

7. Spurny, K.R., Gentry, J.W. and Stoeber, W. "Fundamentals of Aerosol Science", (D.T. Shaw,Ed). Chap 5, Wiley, New York,1978.

8. Brenner, H. and Condiff, D.M.J. Colloid Interface Sci. 47,199 (1974); where further numerous references are given.

9. Prager, S. Trans. Soc. Rheol.1, 53 (1957)

10. Peterlin, A.Z. Phys 111,232 (1938)

11. Stewart, W.E. and Sorensen J.P. Trans. Soc. Rheol.16, 1 (1972)

12. Takserman-Krozer, R. and Ziabicki, A., J. Polym.Sci. A 1.491 (1963).

13. Rallison, J.M.J. Fluid Mech. 84 ,237 (1978).

14. Hinch E.J. and Leal.L.G.J. Fluid Mech.76,187 (1976).

15. Jeffery, G.B. Proc.Roy.Soc. A 102,161 (1923)

16. Hinch, E.J. and Leal, L.G.J. Fluid Mech.92,591 (1979)

17. Gans R., Ann Phys.86,628 (1928).

18. Burlish,R. and Stoer,J. Num.Math.8, 1 (1966).

19. Schlichting H. "Boundary Layer Theory," p. 220 Mc-Graw-Hill, New York 1968.

III THE TURBULENT CLOUD CASE

1. The (Theoretical) Models

Having performed a study on the orientation density function (o.d.f.) of small spheroidal aerosol particles in a general field of an arbitrary strength, (1,2) it became possible to treat the orientation problem in a turbulent medium. To this end, two interconnected physical models were applied. In the <u>first</u>, "The Realizations Model," it was assumed that the turbulent particle field constituted an ensemble of an infinite number of realizations, j, each one of which is characterized by one set of the o.d.f., $F^{(j)}(x,t)$ values. The latter was taken in that model to essentially coincide with the previously found solution of the Fokker-Planck equation (1,2) in the field of the realization

$$\frac{\partial F^{(j)}}{\partial t} + \nabla \cdot \left[\omega(W_{ik}^{(j)}, R) F - \alpha_e^{-1(j)} \nabla F^{(j)} \right] = 0 \qquad (3.1)$$

where ω is the rotational velocity of the particles and $\alpha_e^{(j)}$ is their rotational Peclet number defined by $W_0 / {}^r D_e$, W_0 being a typical component of the (fluid) gradient tensor, ${}^r D_e$ an effective rotational diffusion coefficient and R the particle aspect ratio ; $W_{ik}^{(j)}$ is a gradient component $\delta u_i / \delta x_k$ (u_i - a component of the fluid velocity). The use of the solution is based on the estimate that, even for the highest (Kolmogoroff) frequency component of u_i, the rotational Reynolds number for the studied particles is small enough to render their motion (quasi)stationary.

In the <u>second</u>,"The Micro-turbulence Model," a relation between the so-called turbulent diffusion coefficient ${}^r D_t$ of the particles and the physical characteristics of the fluid field was supplied. This coefficient and the Brownian rotational diffusion one, ${}^r D_B$, compose the effective diffusion coefficent ${}^r D_e$

$$^r D_e = {}^r D_t + {}^r D_B . \qquad (3.2)$$

Expressing the stochastic quantities of the system as $F = \overline{F} + F', \omega_i = \overline{\omega}_i + \omega_i', W_{ik} = \overline{W}_{ik} + W_{ik}'$ and $u_i = \overline{u}_i + u_i'$, it could be shown that the realizations average of F,F($W_{ik}^{(j)}, {}^r D_B, R$) for a space-time point is actually $F(\overline{W}_{ik}, {}^r D_e, R)$ for that point and that

$$\overline{\omega' F'} = -{}^r D_t \, \nabla \overline{F} . \tag{3.3}$$

The particles considered were taken to be much smaller than the Kolmogoroff scale; so, the turbulent rotational diffusion coefficient itself, ${}^r D_t$, was assumed, in the second model, to depend on the randomizing action of the turbulent pressure fluctuations at the particles' surface which arise from the (Kolmogoroff) micro-turbulence.

From dimensional analysis it was obtained that

$$^r D_t \approx (\varepsilon / \nu)^{1/2} \tag{3.4}$$

where ε , the turbulent dissipation energy, is given for a homogenous field by (3)

$$\varepsilon = \nu \sum_{ik} \overline{W_{ik}'^2} \tag{3.5}$$

2. Applications

As the turbulent gradient tensor W_{ik}' is not completely known in many fluid systems, it was necessary in the present study either to supplement the missing data by the results of numerical simulations or (reasonable)guesses or both. In cases of interest, there was conducted a _parametric_ investigation in which the effect of structure changes in the gradient tensor on the o.d.f. was tested.

The numerical simulations of the turbulent field were carried out according to the method of Wang and Frost (4) where $u_i' = u_i'(t)$ is found. In this method, however, only the three components W_{i1}' (i= 1,2.3) could be acquired due to the applicability of the relationship known as the Taylor hypothesis, viz.

$$\frac{\delta u_i}{\delta t} = -\overline{u}_i \frac{\delta u_i}{\delta x_1} \tag{3.6}$$

to those components alone.

Results

Two physical situations were studied:

1. The near-ground atmospheric boundary layer, in which only

$$\overline{u}_1(z) = \frac{u^*}{k_o} \ln\left(1 + \frac{z}{z_o}\right) \tag{3.10}$$

and

$$\overline{W}_{13} = \frac{\delta \overline{u}_1}{\delta z} = \frac{u^*}{k_o(z + z_o)} \tag{3.11}$$

essentially exist, z being the elevation above ground, $\overline{u}_1$ the mean horizontal velocity, u^* the friction velocity, k_o von Karman constant and z_o the roughness height.

2. The turbulent round free jet, for which the Schlichting's solution for the average velocity components (7) was used. In this solution, the (molecular) kinematic viscosity ν is replaced by a virtual (turbulent) kinematic viscosity ε_o given in the equation

$$\varepsilon_o = 0.161 \, J'^{1/2} \tag{3.12}$$

where $J' \, (= J/\rho) = 1.59 \, b_{1/2} \overline{u}_o$, J' is the kinematic momentum of the jet, $b_{1/2}$ is its half-width and $\overline{u}_o$ is the average fluid velocity along its axis ($b_{1/2} = c \, x_1$ in which c is 0.63 to 0.79, as experimentally found).

In the boundary layer situation, both the case of a "weak turbulence", where $W_o' \approx \overline{W}_o$, and a "strong turbulence", where $W_o' \gg \overline{W}_o$ were investigated.

For the first case, numerical simulations were employed while for the second one Klebanoff's experimental data (5) supplemented by simulations was applied. Also, in the latter case, the version

$$\overline{W_{32}'^2} = \overline{W_{23}'^2} = \overline{W_{13}'^2} \tag{3.13a}$$

or

$$\overline{W_{32}'^2} = \overline{W_{23}'^2} = \overline{W_{11}'^2} \tag{3.13b}$$

was taken. The calculations in both cases were carried out with $\nu=0.15$ cm^2/sec., δ (thickness of the atmospheric boundary layer)$= 10^3 m$, $z_o = 0.1 m$, $k_o = 0.4$, $^rD_B = 1 sec^{-1}$ and ϵ deduced from Eq. (5). The calculation time for $\overline{F}$ was greater than the relaxation time of the particles, and $\Delta\theta = \Delta\varphi = \pi/12$ or $\pi/24$.

In the turbulent jet situation, the ratio between the various values of $\overline{W_{ik}'^2}$ was obtained (6) through

$$c_2 \overline{W_{ii}'^2} = \overline{W_{ki}'^2} \quad (i,k, = 1,2,3 ; \; i = k) \tag{3.14}$$

where $c_2 = 1 + exp(-200r^2)$, r being the radial distance within the jet.

For both situations, the absolute values of $\Delta W_{ik}'$ were deduced by normalization according to Eq.(3.5). Values of $\overline{F}$, and F_m, together with the deviations of F for fields (2)&(3) (above), were calculated as a function of height above ground (and hence ϵ) in the boundary layer situation, the aspect ratio of the particles, R (R>1 for fibers and R<1 for platelets), and the parameterization factor α_o. However, only the following typical figures were presented here:
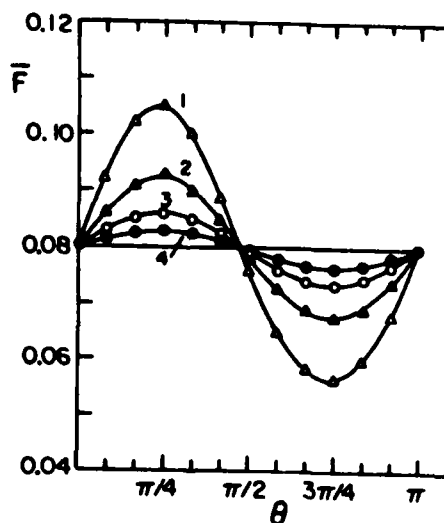

Fig.1. The average o.d.f., $\overline{F}$,vs. θ for the
atmospheric boundary layer, "weak turbu-
lence", with :
z = 2.5 to 20m;(1)2.5m,(2)5m,(3)10m,(4)20m
R = 10 , $\varphi_m = \pi/2$,
$\alpha_e = 1, \overline{W_{13}}(=\overline{W_o})$ according to Eq.(3.11) , $W_o' = \Delta W_{13}'$.
Solid lines are simulation results (254 realizations, usually); points are values
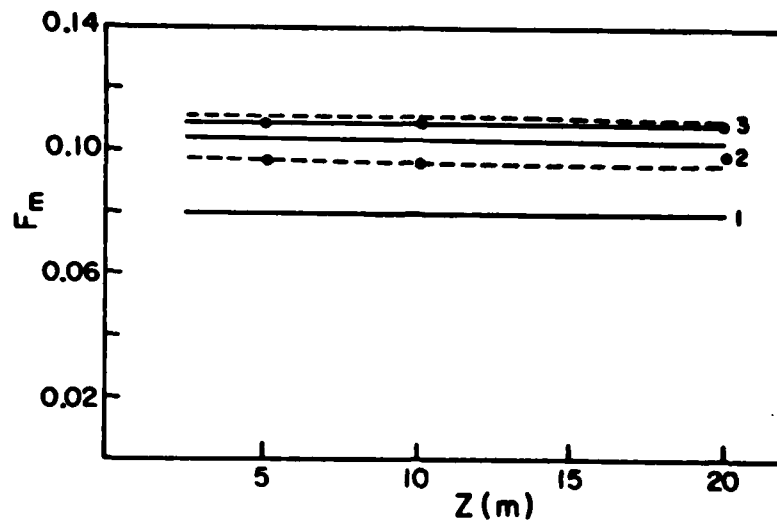calculated from the $\overline{W_{ik}}$ field.

Fig.2. The maximal o.d.f. F_m, vs. height for the atmospheric boundary
layer, "strong turbulence", $R = 50$; ε decreases with height accor-
ding to Ball (8). (1) $W_{ik}^{(1)}$, (2) $W_{ik}^{(2)}$, (3) $W_{ik}^{(3)}$; dashed
lines are cases where terms of Eq.(3.7) are taken with opposite signs;
points relate to combination of Eq. 3.13b (Line 1 essentially
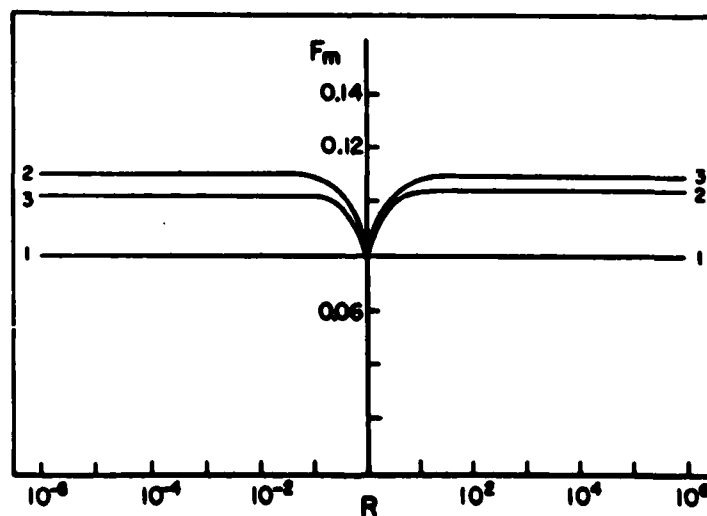coincides with the random distribution one).

Fig. 3. The maximal o.d.f., F_m vs. particle aspect ratio R for the
atmospheric boundary layer, "strong turbulence".

$z = 5m$, $\varepsilon = 230$ cm^2/sec^{-3}

(1) $W_{ik}^{(1)}$,(2) $W_{ik}^{(2)}$, (3) $W_{ik}^{(3)}$

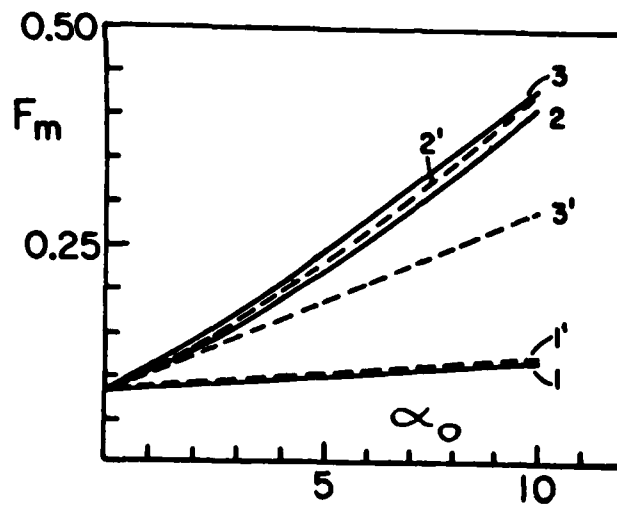(Line 1 essentially coincides with the random distribution one).

Fig. 4. The maximal o.d.f. F_m vs. the parameter α_o for the atmospheric boundary layer; "strong turbulence".

$R = 50$ ——— ; $R = 0.02$ — — — ; $z = 2.5m$; $\varepsilon = 5 cm^2/sec^3$.

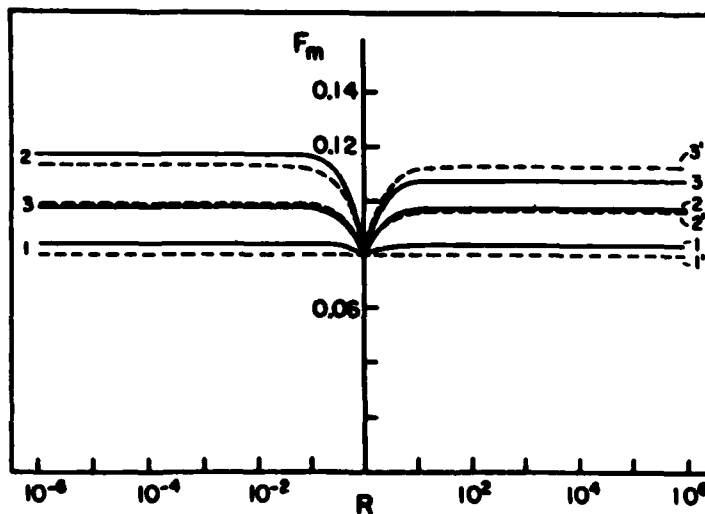(1) $W_{ik}^{(1)}$, (2) $W_{ik}^{(2)}$, (3) $W_{ik}^{(3)}$

Fig. 5. The maximal o.d.f., F_m vs. particle aspect ratio R for a free turbulent jet.

Locations: $x_1 = 2$, $x_2 = x_3 = 0.05$ (see ref.1),

$\overline{W}_o = 5$ sec^{-1}, $\varepsilon = 250$ cm^2/sec^3

(1),(1'): $W_{ik}^{(1)}$;(2),(2'): $W_{ik}^{(2)}$;(3),(3'): $W_{ik}^{(3)}$ for (1'),(2'),(3') terms of Eq (3.7) are taken with opposite signs. (Line 1 essentially coincides with the random distribution one)
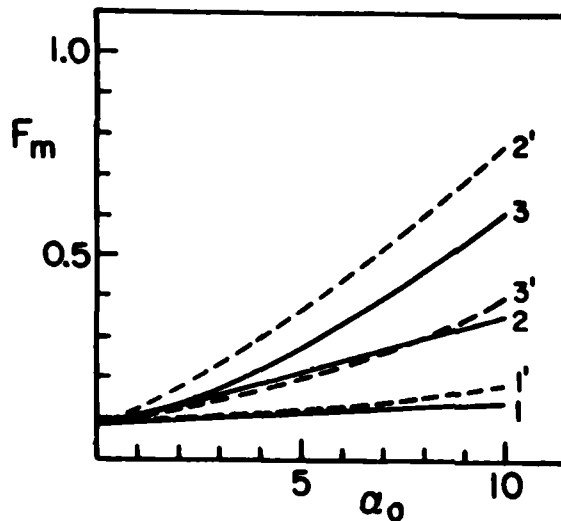
Fig. 6. The maximal o.d.f., F_m vs. the parameter α_o for a free turbulence jet.

$$\overline{W_o} = 5 \sec^{-1}$$
$$\epsilon = 125 \text{ cm}^2/\sec^3 \quad ; \quad R=50 \quad \begin{array}{l} x=2, x_2 = x_3 = 0.05 \text{ (see ref.1)} \\ \hline \end{array} , R = 0.02 \; - - - -$$

3. Interim Conclusions

Atmosphere boundary layer (up to 20 m height):

1. The average o.d.f. in a weak turbulent field shows structured (preferred) orientation;

2. The maximal (and average) o.d.f. in a strong commonly occurring, turbulent field of the average realization $W_{ik}^{(1)}$ essentially coincides with the random distribution while the spread of the values of the function between fields $W_{ik}^{(2)}$ and $W_{ik}^{(3)}$ is quite significant. This spread of values may have practical connotations.

3. The values of F_m and its deviations increase with the parameter α_o as expected.

Free turbulent jet:

Conclusions 2 and 3 of the former situation apply here too.

APPENDIX   C: REFERENCES

1. E.M. Krushkal and Isaiah Gallily, J. Colloid Interface Sci. 99, 141 (1984).

2. Isaiah Gallily and E.M. Krushkal, Proceedings of the 1983 CSL Conference on Obscuration and Aerosol Research.

3. Hinze, J.O., "Turbulence, "McGraw-Hill, Inc. (1975).

4. Wang S.T., and Frost, W., NASA   CR 3309 (1980).

5. Klebanoff, P.A., NACA TN 3178 (1954).

6. Wignansky, I., and Fiedler, H., J. Fluid Mech. 38, 577 (1969).

7. Schlichting, H., "Boundary Layer Theory", McGraw-Hill Inc. (1968) pp.220,699.

8. Bell, F.K., J. Meteorol., 18, 553 (1961).

IV. EXPERIMENTAL

1.Method

The experimental method consisted of a determination of a physical effect from which the orientation density functions (o.d.f.) F of the particles can be deduced.

Light scattering was chosen to be that effect. Thus, the method adopted by us was essentially an inversion of the signal-integral

$$\overline{I} = \int_{0}^{2\pi} \int_{0}^{2\pi} \int_{0}^{\pi} \int_{l} \int_{r} I(\eta, \lambda, l, r, \varphi, \psi, \theta, \beta) f(r) g(l) F(\theta, \varphi, \psi)$$

$$dr\, dl\, \sin\theta\, d\theta\, d\varphi\, d\psi$$

$$(4.1)$$

where $\overline{I}$ is an average (measured) light intensity at an angle β from the initial direction of its propagation , $f(r)$ and $g(l)$ are distribution functions of characterizing geometric parameters of the particles (r-radius, 1-length for cylinders), and φ, θ, ψ are Eulers' angles (ψ disregarded for centrally axi-symmetric particles).

Here, as one did expect that in a turbulent field particle orientation F will fluctuate, we planned to also determine the (central) variance of the signal, $\overline{I_{0}^{2}}$, given by

$$\overline{I_{0}^{2}} = \int_{0}^{2\pi} \int_{0}^{2\pi} \int_{0}^{\pi} \int_{l} \int_{r} (I - \overline{I})^{2} f(r) g(l) F(\theta, \varphi, \psi)$$

$$dr\, dl\, \sin\theta\, d\theta\, d\varphi\, d\psi$$

$$(4.2)$$

It should be remarked that the dependability of this method in extracting a sufficiently accurate values of the o.d.f.   F from the signal integrals (4.1) and (4.2) hinges on the pre-knowledge of f (r) and g(1). So, envisaging some experimental difficulties in this direction, we launched an independent

(and financially unsupported) study of a direct determination of F.

2. Apparatus

General considerations

The experiments were conducted in the fully-developed turbulent region of a straight, horizontal round pipe where quiet a bulk of characterizing information exists (1). Thus, for the (round) pipe geometry, one has that in a fully developed flow (1)

$$\left. \begin{array}{l} \bar{u}_r , \ \bar{u}_\varphi = 0, \\[2mm] \partial/\partial\varphi = 0, \\[2mm] u_x , \ u_r , \ u_\varphi \neq f(x) \end{array} \right\} \qquad (4.3)$$

and

where x is the coordinate along the average flow, and u_x, u_r, u_φ are respectively the velocity components in the x,r (the radial) and φ (the azimuthal) directions.

Also, one has

$$\overline{u'_r \, u'_\varphi} = 0 \quad \text{for all } r \qquad (4.4)$$

where the prime symbol signifies the fluctuating part of the components.

Specific

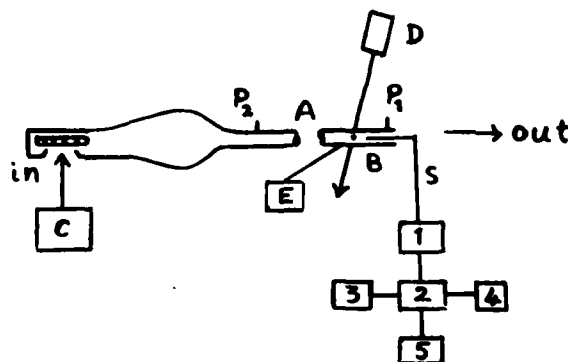A schematic diagram of the apparatus is shown in Fig. 1-

Fig.1. The apparatus (schematical)

in which

A is a 5 m long, 5 cm. i.d. cylindrical tunnel,

B is an aerosol observation section,

C is Spurney's fiber aerosol generator,

D is a light source,

E is (scattered) light detector (EMI photomultiplier type 9558) and read-out,

P_1 P_2 are aerosol sampling ports.

S is a 3 D (or 2 D X -wire) sensor (TSI, Model 1295 -T1.5) including:

1. CTA supplier and linearizer (Disa, 56N21 with 56 C16 Bridges)

2. Mini computer (Digital, LSI/11/23 +,250 K samples/sec)

3,4,5 - Diskette drive (SMS, FWTO122S), printer (FACIT) monitor (Visual 102).

3. Aerosol

The aerosol used consisted of glass fibers produced by the Spurny
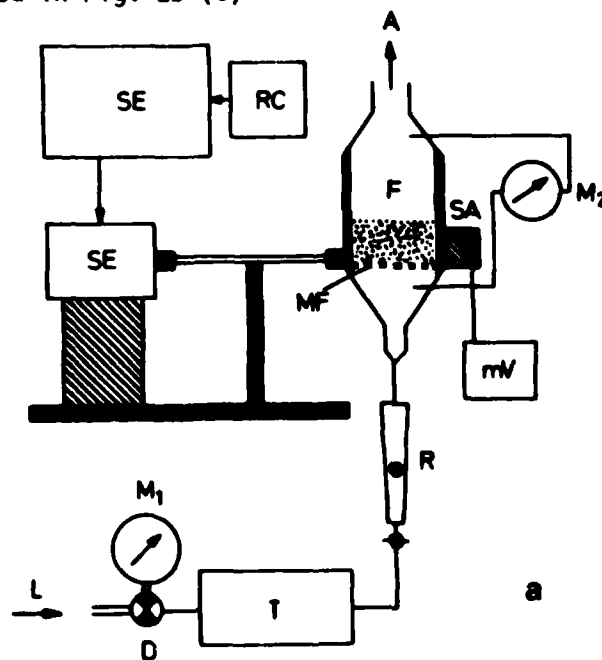generator (Fig.2a) (2); a typical size distribution of the fibers is
presented in Fig. 2b (3)

Fig. 2a. The Spurny generator (schematical)
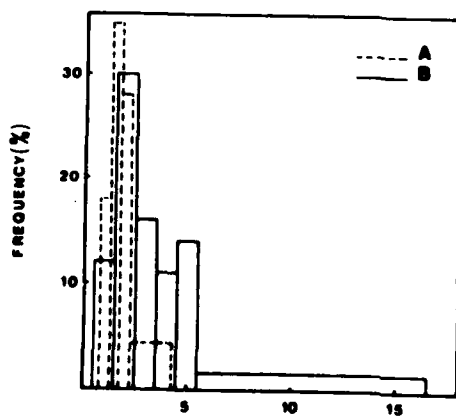F-container of fibers' mass; SE,RC=electromechanical device .

Fig. 2b. A typical size distribution of the glass fibers..
A - diameter $\times 10^{5}$ cm, B - length $\times 10^{4}$ cm

4. Experimental Procedure

Setting the average air flow through the tunnel at a certain value befitting, say, an average Reynolds number of 10^{4}, the turbulent velocity components along the x and r coordinates are sampled at a prescribed rate by the (computerized) system 1-4 (Fig.1)and the data processed for $\overline{u_x'^2}$, $\overline{u_r'^2}$, $\overline{u_x' u_r'}$ .The necessary gradients (see Part III of this report), say $[\overline{(\partial u_r'/\partial r)^2}]^{1/2}$, can be deduced from:

1. The Taylor hypothesis

$$\partial u_x'/\partial t = -\overline{u}_x \frac{\partial u_x'}{\partial x} , \qquad (4.5)$$

2. The incompressibility demand,

3. Supplementary values taken from Laufer (1) for the dissipation terms,

4. The isotropic conditions assumed to hold far from the walls of the flow tunnel (1).

Then, the aerosol generator is operated and aerosol samples taken through portholes P_1, P_2 (FIG.1) with the aid of a (Cassela) thermal precipitator for a scanning electron microscope analysis. The (aerosol) collecting surface within the precipitor is wetted before sampling to obviate the need for photogrammetry (4).

Finally, scattered light signals are taken.

Results are being accumulated now.

V. SUMMARY

A theoretical method has been developed for the calculations of the orientation density function of elongated and flat aerosol particles subjected to the most general laminar flow or to a turbulent field.

Some typical situations such as a point source flow, a laminar round jet flow, the (lower)atmospheric (turbulent) boundary layer and the turbulent round jet, were specially treated.

An experimental apparatus essentially consisting of an horizontal (pipe) wind tunnel has been constructed to check the theoretical results through the effect of particle orientation on light scattering. The apparatus, equipped with a (dedicated) very fast computerized system, is functioning smoothly. Scattered light readings are being taken.

APPENDIX D : REFERENCES

1. J. Laufer, "The Structure of Turbulence in Fully Developed Pipe Flow," NACA Report 1174, 1954.

2. Spurny, K.R. et al., Staub Reinhalt Luft 35, 440 (1975).

3. A.D. Eisner and Isaiah Gallily, J. Colloid and Interface Sci. 101, 356 (1984).

4. Isaiah Gallily, J. Colloid and Interface Sci. 37, 403,(1971).

END
FILMED

6-86

DTIC